J. Fluid Mech. (1982), *vol.* 119, *pp.* 155–172
Printed in Great Britain

On the accuracy of turbulence measurements with inclined hot wires

By UDO R. MÜLLER
Aerodynamisches Institut, Technische Hochschule Aachen, West Germany

(Received 18 September 1980 and in revised form 28 October 1981)

Since the accuracy of mean velocities and Reynolds stresses measured with inclined hot wires depends on the accurate knowledge of the hot-wire cooling law, each hot wire used in the boundary-layer experiment of Müller (1982, hereinafter referred to as I) had to be calibrated individually with respect to the magnitude and direction of the flow vector. In the present paper details of the calibration procedure and an example of calibrated data are reported. The directional hot-wire response was described by an effective cooling velocity, which was then used for the data reduction. The errors in the measured Reynolds stresses evaluated with an empirical cooling law as opposed to the actual one were estimated analytically from the governing equations and were confirmed by corresponding recalculations from the same set of measurements. Additionally, the validity of the conventional linearized method for evaluating the Reynolds stress tensor from the root-expanded equation for the cooling velocity was checked for increasing turbulence levels. In the test measurements all triple velocity correlations, which are usually neglected compared with second-order ones, were measured and taken into account in the data reduction.

1. Introduction

Most present prediction methods for turbulent boundary-layer flows use the time-averaged Reynolds equations. The unknown Reynolds stresses have to be described by an empirical turbulence model adapted to the type of flow considered. Refinements of present models in order to develop computational methods for complex flow fields including for example strong adverse pressure gradients or separated and reattached regions are achieved mainly by measuring the mean and fluctuating flow field of specially designed experiments (Marvin 1977). Thus the 'fact gap' (Bradshaw 1972) between computational capacity and experiments suitable to guide flow-field predictions can be decreased.

The development of numerical methods for calculating three-dimensional turbulent boundary layers has been advanced intensively in recent years, in order, for example, to support the design of swept wings with low aspect ratio. However, the turbulence structure of three-dimensional flows is still not well understood. Experiments in incompressible boundary layers with pressure-driven secondary flow, for example those of van den Berg & Elsenaar (1972) and Elsenaar & Boelsma (1974), Dechow (1977), and Johnston (1970) indicated that a simple application of turbulence models developed for two-dimensional flows is generally not valid. As Rotta (1977) pointed out, the anisotropy of closure assumptions has to be taken into account in prediction

methods. This was confirmed by the calculations of Krause (1974, 1975) and Kordulla, when compared to the infinite-swept-wing experiment of van den Berg, Elsenaar and Boelsma; the predictions of the three-dimensional boundary layer were sensitive to the assumed closure of the crosswise momentum equation.

Since only a few experiments in three-dimensional turbulent boundary layers are suitable for the verification and refinement of turbulence models for these flows, a pressure-driven incompressible turbulent boundary layer over a plane wall developing from two-dimensional to fully three-dimensional conditions was investigated. As reported in I profiles of the mean velocities and of the Reynolds stress tensor as well as the wall shear stresses and the pressure distribution were measured. By means of a probe support similar to that proposed by Johnston (1970) an X-hot-wire probe was aligned with the local yaw direction and then rotated around the longitudinal axis in order to measure all Reynolds stresses locally. In preliminary experiments this method was checked by repeated measurements of profiles of the Reynolds stress tensor using three nominally identical X-wire probes. With each probe orientated at four angular positions, a total of 48 r.m.s. measurements was obtained per measuring point. Redundant evaluations of the Reynolds stress tensor from different sets of measurements, however, indicated large scatter, especially for the important crosswise shear stress. While keeping typical error sources of the hot-wire measurements small, we found that the correct description of the hot-wire response to the flow direction was crucial to the accuracy of the results. The cooling of the hot wires used could not be described by a single cooling law, so each wire had to be calibrated individually with respect to the magnitude and direction of the flow vector. By incorporating the calibrated data in the evaluation of the Reynolds stresses the accuracy of the results was improved.

Since in the flow field of I the local tubulence levels increased appreciably with decreasing distance from the separation line, we expected limitations on the use of the conventional linearized method for evaluating the Reynolds stress tensor. The applicability of this method, which neglects triple-order velocity correlations compared with second-order ones, was checked in the vicinity of separation with turbulence levels up to 35 %. By including all measured triple velocity correlations in the data reduction and neglecting the fourth-order terms, the calculated Reynolds stresses could be compared with those evaluated conventionally.

2. Data-reduction method for low turbulence levels

2.1. *Linearized hot-wire response equations*

In the boundary-layer experiment described in I, the yaw direction and magnitude of the local, resultant mean-velocity vector were determined using a single normal hot wire orientated parallel to the wall; the yaw direction defined the measuring coordinate system (x_m, y_m, z_m) in figure 1. Then an X-hot-wire probe was placed in the (x_m, y_m)-plane similar to the single-wire probe sketched in the figure, and the mean-velocity component V_m normal to the wall was determined; although the accuracy of this measurement was known to be limited by mean velocity gradients in the near-wall region. A sufficient number of measurements for evaluating all components of the local Reynolds stress tensor was obtained by rotating the X-probe with prescribed

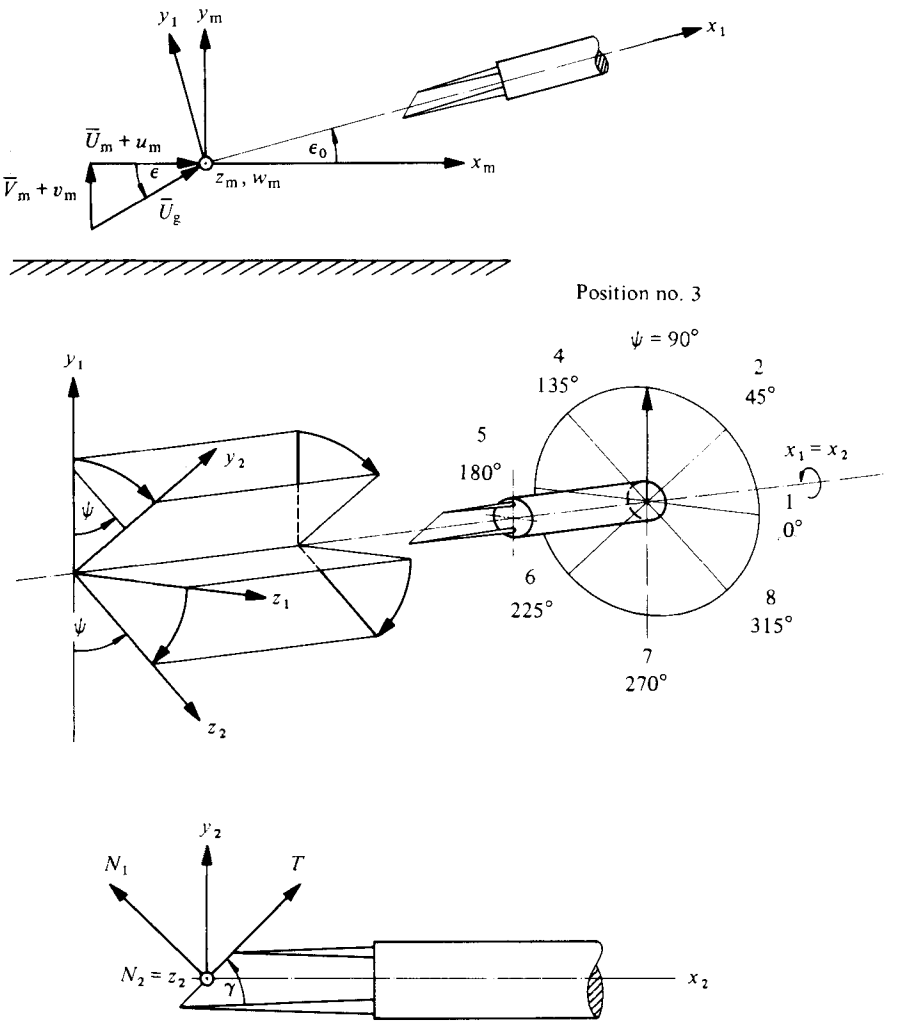

FIGURE 1. Transformation of streamline co-ordinate system (x_m, y_m, z_m) onto hot-wire fixed system (N_1, T, N_2).

intervals around the longitudinal axis, thus placing the wires at different orientations relative to the velocity field (e.g. Hinze 1975; Champagne, Sleicher & Wehrmann 1967; Elsenaar & Boelsma 1974; Dechow 1977; Vagt 1979). The corresponding equations used in I for evaluating the mean and fluctuating velocities from the hot-wire measurements will be briefly derived in this section.

The cooling of an ideal hot wire of infinite length in a three-dimensional flow depends on the velocity components normal to the wire axis ('cosine law'). In practice, however, the response to the flow direction is increasingly affected with decreasing ratio of wire length to diameter, for example, by heat conduction and aerodynamic disturbances caused by the prongs. Also manufacturing imperfections like wire slack yield deviations from an ideal cooling law. For the present investigation Jörgensen's (1971) cooling law describing the hot-wire response in a three-dimensional laminar flow by

means of an effective cooling velocity was assumed to be valid instantaneously in a turbulent flow, so that

$$\left(\frac{E}{S}\right)^2 = \left(\frac{\bar{E}+e}{S}\right)^2 = U_c^2 = (\bar{U}_{N1}+u_{N1})^2 + k^2(\bar{U}_T+u_T)^2 + h^2(\bar{U}_{N2}+u_{N2})^2. \tag{1}$$

The output voltage E of an analogue linearizer circuit was related to the cooling velocity U_c by the calibration constant S. The mean-velocity components $\bar{U}_{N1}$ and $\bar{U}_T$ were perpendicular and tangential to the wire in the plane of the prongs, $\bar{U}_{N2}$ was perpendicular to both. The fluctuations of voltage and each velocity component are denoted by lower-case letters. The evaluation of the directional sensitivities k and h will be discussed later, they are treated as known constants in this section.

The mean and fluctuating velocities in (1) were described in terms of the velocities $\bar{U}_m+u_m$, $\bar{V}_m+v_m$, w_m of the measuring co-ordinate system by transforming the latter ones onto the hot-wire-fixed co-ordinate system (N_1, T, N_2) using the intermediate systems (x_1, y_1, z_1) and (x_2, y_2, z_2), as illustrated in figure 1. The cooling velocity U_c was obtained as

$$U_c = U_c(\bar{U}_m, \bar{V}_m, u_m, v_m, w_m, \epsilon_0, \gamma, \psi, k, h), \tag{2}$$

where ϵ_0 was the angle between the probe axis and the wall, and γ was the angle between the hot-wire and the probe axis. The roll angle ψ and the corresponding indication of the measuring positions are defined in figure 1. With subscript n indicating the roll angle, and with the other parameters prescribed, the relation between output voltage and velocities becomes

$$E_n^2/S^2 = U_{cn}^2 = \bar{F}_n^2[(\bar{U}_i\bar{U}_j)_m] + f_n[(\bar{U}_i, u_i)_m] + g_n[(u_iu_j)_m]. \tag{3}$$

$\bar{F}^2$ and g contain all double velocity correlations of mean and fluctuating velocity components respectively; f includes the linear fluctuation terms. With the definitions

$$\left.\begin{aligned} A &= \cos\epsilon_0 \sin\gamma + \sin\epsilon_0 \sin\psi \cos\gamma, \\ B &= \sin\epsilon_0 \sin\gamma - \cos\epsilon_0 \sin\psi \cos\gamma, \\ C &= \cos\epsilon_0 \cos\gamma - \sin\epsilon_0 \sin\psi \sin\gamma, \\ D &= \sin\epsilon_0 \cos\gamma + \cos\epsilon_0 \sin\psi \sin\gamma \end{aligned}\right\} \tag{4}$$

$\bar{F}^2$, f and g are

$$\begin{aligned} \bar{F}^2 = \bar{U}_m^2(A^2 + k^2C^2 + h^2\sin^2\epsilon_0\cos^2\psi) + \bar{V}_m^2(B^2 + k^2D^2 + h^2\cos^2\epsilon_0\cos^2\psi) \\ + 2\bar{U}_m\bar{V}_m(AB + k^2CD - h^2\sin\epsilon_0\cos\epsilon_0\cos^2\psi), \end{aligned} \tag{5}$$

$$\begin{aligned} f = {} & u_m(2\bar{U}_m(A^2 + k^2C^2 + h^2\sin^2\epsilon_0\cos^2\psi) \\ & + 2\bar{V}_m(AB + k^2CD - h^2\sin\epsilon_0\cos\epsilon_0\cos^2\psi)) \\ & + v_m(2\bar{U}_m(AB + k^2CD - h^2\sin\epsilon_0\cos\epsilon_0\cos^2\psi) \\ & + 2\bar{V}_m(B^2 + k^2D^2 + h^2\cos^2\epsilon_0\cos^2\psi)) \\ & + w_m(2\bar{U}_m(-A\cos\psi\cos\gamma + k^2C\cos\psi\sin\gamma + h^2\sin\epsilon_0\cos\psi\sin\psi) \\ & + 2\bar{V}_m(-B\cos\psi\cos\gamma + k^2D\cos\psi\sin\gamma - h^2\cos\epsilon_0\cos\psi\sin\psi)), \end{aligned} \tag{6}$$

$$g = u_m^2(A^2 + k^2C^2 + h^2\sin^2\epsilon_0\cos^2\psi) + v_m^2(B^2 + k^2D^2 + h^2\cos^2\epsilon_0\cos^2\psi)$$
$$+ w_m^2(\cos^2\psi\cos^2\gamma + k^2\cos^2\psi\sin^2\gamma + h^2\sin^2\psi)$$
$$+ u_m v_m 2(AB + k^2CD - h^2\sin\epsilon_0\cos\epsilon_0\cos^2\psi)$$
$$+ u_m w_m 2(-A\cos\psi\cos\gamma + k^2C\cos\psi\sin\gamma + h^2\sin\epsilon_0\cos\psi\sin\psi)$$
$$+ v_m w_m 2(-B\cos\psi\cos\gamma + k^2D\cos\psi\sin\gamma - h^2\cos\epsilon_0\cos\psi\sin\psi). \quad (7)$$

The final equations were obtained after separating the mean and fluctuating parts of the cooling velocity by means of a binomial expansion of (3):

$$\frac{\bar{E}_n}{S} = \bar{U}_{cn} = \bar{F}_n + \frac{\bar{g}_n}{2\bar{F}_n} - \frac{\overline{f_n^2}}{8\bar{F}_n^3} + O(\overline{u_i^3}), \quad (8)$$

$$\overline{\left[\frac{e_n}{S}\right]^2} = \overline{\left[\frac{E_n - \bar{E}_n}{S}\right]^2} = \frac{\overline{f_n^2} + 2\overline{f_n g_n}}{4\bar{F}_n^2} - \frac{\overline{f_n^3}}{8\bar{F}_n^4} + O(\overline{u_i^4}), \quad (9)$$

$$\frac{\overline{(e_n \pm e_{n+4})^2}}{S^2} = \frac{1}{4}\left[\overline{\left[\frac{f_n}{\bar{F}_n} \pm \frac{f_{n+4}}{\bar{F}_{n+4}}\right]^2} + 2\overline{\left[\frac{f_n}{\bar{F}_n} \pm \frac{f_{n+4}}{\bar{F}_{n+4}}\right]\left[\frac{g_n}{\bar{F}_n} \pm \frac{g_{n+4}}{\bar{F}_{n+4}}\right]}\right]$$
$$- \frac{1}{8}\overline{\left[\frac{f_n}{\bar{F}_n} \pm \frac{f_{n+4}}{\bar{F}_{n+4}}\right]\left[\frac{f_n^2}{\bar{F}_n^3} \pm \frac{f_{n+4}^2}{\bar{F}_{n+4}^3}\right]} + O(\overline{u_i^4}). \quad (10)$$

The mean square of the sum and difference of two signals has to be measured by means of an X-wire-probe with wires in positions n and $n+4$ respectively. For measurements in flows with low turbulence intensity (about 10 %) all fluctuation terms in (8) and all terms higher than second order in (9) and (10) are neglected and the final equations for determining the components of the mean flow vector and of the Reynolds stress tensor are retained.

In I 16 r.m.s. measurements according to (9) and (10) were carried out at four angular positions at each measuring point. The spatial resolution and the accuracy of the measurements as well as the influence of non-constant directional hot-wire sensitivities k and h were checked by evaluating the Reynolds stress tensor with three different sets of equations. The leading terms were obtained after simplifying (4)–(10) by setting $\epsilon = \epsilon_0 = k = 0$, $h = 1$ and $\gamma = 45°$; the simplified equations are summarized in table 1. The results of I were calculated by inverting the complete 6×6 matrices and arithmetically averaging the solutions.

2.2. *Directional hot-wire sensitivities*

In I the Reynolds stresses and the normal velocity $\bar{V}_m$ were measured with DISA miniature X-hot-wire probes 55P61. They were chosen in order to measure as close to the wall as possible for resolving the peaks in the profiles of the Reynolds stresses. We used unplated, platinum-coated tungsten wires with $d = 5\,\mu$m and $l = 1{\cdot}2$ mm throughout the measurements. Since the knowledge of each hot wire's directional response according to (1) was required for the data reduction, a calibration device was developed which allowed an arbitrary, accurate positioning of a hot wire relative to the velocity vector of a TSI calibrator (turbulence level $Tu \simeq 0{\cdot}002$). The two-dimensional case is sketched schematically in figure 2 and will be discussed first.

System (*a*)

$$\frac{\overline{(e_3+e_7)^2}}{S^2} = 2\overline{u_m^2},$$

$$\frac{\overline{(e_3-e_7)^2}}{S^2} = 2\overline{v_m^2},$$

$$\frac{\overline{e_3^2}-\overline{e_7^2}}{S^2} = -2\overline{u_m v_m},$$

$$\frac{\overline{(e_1-e_5)^2}}{S^2} = 2\overline{w_m^2},$$

$$\frac{(\overline{e_2^2}-\overline{e_4^2})+(\overline{e_6^2}-\overline{e_8^2})}{S^2} = 2\overline{v_m w_m},$$

$$\frac{(\overline{e_2^2}-\overline{e_4^2})-(\overline{e_6^2}-\overline{e_8^2})}{S^2} = -2\sqrt{2\overline{u_m w_m}}.$$

System (*b*)

$$\frac{\overline{(e_3+e_7)^2}}{S^2} = 2\overline{u_m^2},$$

$$\frac{\overline{e_3^2}-\overline{e_7^2}}{S^2} = -2\overline{u_m v_m},$$

$$\frac{\overline{e_1^2}+\overline{e_5^2}}{S^2} = \overline{u_m^2}+\overline{w_m^2},$$

$$\frac{\overline{e_2^2}+\overline{e_4^2}}{S^2} = \overline{u_m^2}+\tfrac{1}{2}\overline{v_m^2}+\tfrac{1}{2}\overline{w_m^2}-\sqrt{2\overline{u_m v_m}},$$

$$\frac{\overline{(e_2-e_6)^2}-\overline{(e_4-e_8)^2}}{S^2} = 4\overline{v_m w_m},$$

$$\frac{\overline{e_1^2}-\overline{e_5^2}}{S^2} = -2\overline{u_m w_m}.$$

System (*c*)

$$\frac{\overline{(e_2+e_6)^2}+\overline{(e_4+e_8)^2}}{2S^2} = 2\overline{u_m^2}, \quad \frac{\overline{(e_3-e_7)^2}}{S^2} = 2\overline{v_m^2}$$

$$\frac{\overline{(e_2-e_6)^2}+\overline{(e_4-e_8)^2}}{S^2} = 2\overline{v_m^2}+2\overline{w_m^2}, \quad \frac{\overline{e_3^2}-\overline{e_7^2}}{S^2} = -2\overline{u_m v_m}$$

$$\overline{v_m w_m} = \tfrac{1}{2}[\overline{v_m w_m}(a)+\overline{v_m w_m}(b)], \quad \overline{u_m w_m} = \tfrac{1}{2}[\overline{u_m w_m}(a)+\overline{u_m w_m}(b)].$$

TABLE 1. Sets of equations used for evaluating the Reynolds stress tensor; simplifications: $\epsilon = \epsilon_0 = k = 0$, $h = 1$ and $\gamma = 45°$

By varying the magnitude $\overline{U}_R$ of the resultant velocity vector as well as the angle α between this vector and the hot-wire normal we found that generally the hot-wire coolings did not obey the empirical relationships suggested in the literature (e.g. Champagne *et al.* 1967; Friehe & Schwarz 1968; Bruun 1975). Additionally, as discussed by Vagt (1979), different results for the tangential sensitivity k of (1) were evaluated, for example by Champagne *et al.* (1967), Jörgensen (1971), Bruun (1971*a*), Kjellström & Hedberg (1970), Irwin (1971) and Horvatin (1970), depending on the type of probe, the wire Reynolds number and the probe orientation to the flow. Therefore it seemed most convenient to use the definition of an effective cooling velocity according to (1) and allow for variable sensitivities. This in turn required an individual calibration of each wire used for the measurements of I.

First the calibration constant S was determined with $\alpha = 0$:

$$\overline{E}(\alpha = 0)/S = \overline{U}_R. \tag{11}$$

Then at angles $\alpha \neq 0$ the tangential sensitivity k was evaluated from

$$k = \left[\left(\frac{\overline{U}_c^2}{\overline{U}_R^2} - \cos^2\alpha\right) \Big/ \sin^2\alpha\right]. \tag{12}$$

One example of the results is given by Müller & Krause (1979), another one for $10° < \alpha < 85°$ and $12\,\mathrm{m/s} \leqslant \overline{U}_R \leqslant 24\,\mathrm{m/s}$ is shown in figure 3. The calibrations with step sizes of $\Delta\alpha = 5°$ proved to be sufficient within the attainable accuracy of the

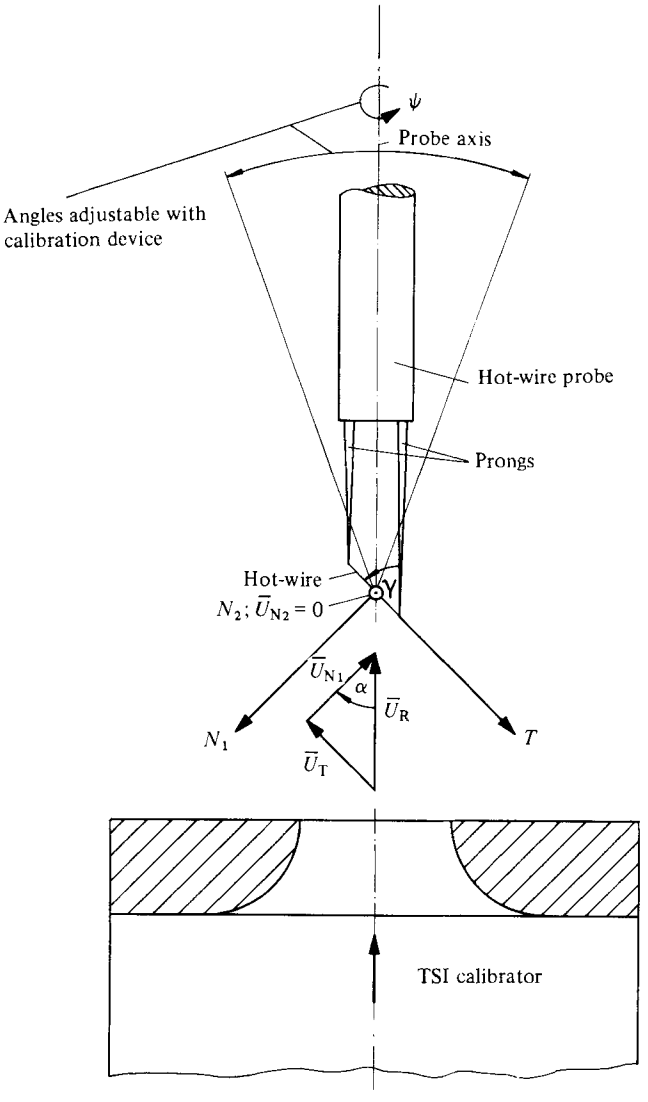

FIGURE 2. Schematic of calibrating the tangential sensitivity k with respect to $\bar{U}_T$.

Reynolds stress measurements of I. Generally the calibrated sensitivities decreased with increasing α for $\alpha < 60°$, where they had minima and depended on the magnitude of the velocity more strongly than at smaller angles. For $\alpha \gtrsim 25°$ the tangential sensitivity increased rapidly, because (12) was not defined for $\alpha \to 0$. For the experiments of I the hot wires had to be calibrated at least in the range $35° \gtrsim \alpha \gtrsim 55°$ indicated by broken lines in figure 3. The velocity range $12\,\mathrm{m/s} \leqslant \bar{U}_R \leqslant 32\,\mathrm{m/s}$ was covered by eight calibrations at each given α, for clarity only four of them are shown in the figure.

The calibrated tangential sensitivities were constant throughout the average lifetime of 20 h of a hot wire. In repeated calibrations with intervals up to 40 h k scattered up to $\pm 10\,\%$, but because of the difficulties in the calibrations themselves as discussed in § 2.3.1 these differences could not be attributed to ageing of the wires.

For measurements in three-dimensional flows relative to the hot-wire probe, the

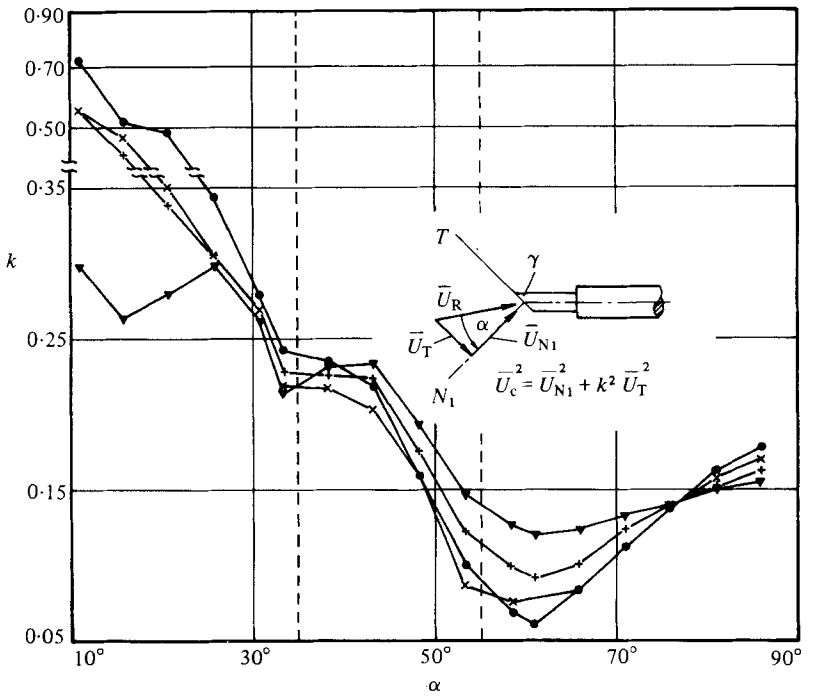

FIGURE 3. Example of calibrated tangential sensitivity k of a hot wire. ▼, $\bar{U}_R$ = 24·0 m/s; +, 17·9 m/s; ×, 13·3 m/s; ●, 12·0 m/s.

velocity $\bar{U}_{N2}$ perpendicular to the plane of the prongs has to be taken into account by a sensitivity h in (1). For the normal-wire probe DISA 55F31 Jörgensen's (1971) calibrations yielded $h \simeq 1{\cdot}1$. In the present calibration of the slanted hot wires used (figure 4) we first aligned the probe axis with the prescribed total velocity vector yielding $\bar{U}_{N2} = 0$, and measured the voltage $\bar{E}(\bar{U}_R)$. Then the plane of the prongs was inclined by an angle σ with respect to the resultant velocity vector which was increased to $\bar{U}_g = \bar{U}_R/\cos\sigma$ in order to retain the cooling by $\bar{U}_R$ measured before. The sensitivity h was calculated from

$$h = \left[\frac{\bar{E}^2(\bar{U}_g) - \bar{E}^2(\bar{U}_R)}{S^2 \bar{U}_g^2 \sin^2\sigma}\right]^{\frac{1}{2}}. \tag{13}$$

The measured results were larger than unity for all hot wires investigated for the range $0 < \sigma < 10°$. But because of scatter, especially for small σ, the data did not show any dependence on angle or Reynolds number and were approximated by an average constant value of $h = 1{\cdot}2$.

The calibrated hot-wire sensitivities had to be taken into account in evaluating the mean velocities and Reynolds stresses from the measurements. The mean velocity $\bar{V}_m$ normal to the wall was determined by means of the angle $\tilde{\epsilon} = \epsilon - \epsilon_0$ between the resultant velocity vector and the probe axis (figure 1), $\epsilon = -\arctan(\bar{V}_m/\bar{U}_m)$. With (5) and (8) and the measured mean voltages $\bar{E}_3$ and $\bar{E}_7$ $\tilde{\epsilon}$ was calculated from

$$\tan^2\tilde{\epsilon} + 2\tan\tilde{\epsilon}\,\frac{\bar{E}_3^2 \sin\gamma_B \cos\gamma_B(1-k_B^2) + \bar{E}_7^2 \sin\gamma_A \cos\gamma_A(1-k_A^2)}{\bar{E}_3^2(\cos^2\gamma_B + k_B^2\sin^2\gamma_B) - \bar{E}_7^2(\cos^2\gamma_A + k_A^2\sin^2\gamma_A)}$$
$$+ \frac{\bar{E}_3^2(\sin^2\gamma_B + k_B^2\cos^2\gamma_B) - \bar{E}_7^2(\sin^2\gamma_A + k_A^2\cos^2\gamma_A)}{\bar{E}_3^2(\cos^2\gamma_B + k_B^2\sin^2\gamma_B) - \bar{E}_7^2(\cos^2\gamma_A + k_A^2\sin^2\gamma_A)} = 0. \tag{14}$$

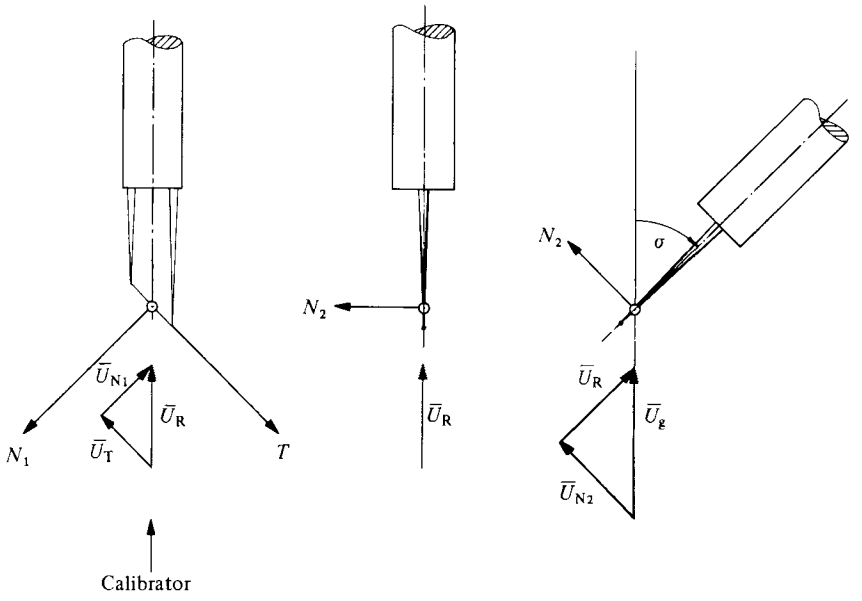

FIGURE 4. Schematic of calibrating the sensitivity h with respect to $\bar{U}_{N2}$.

Only the solution yielding $|\tilde{\epsilon}| < 45°$ made sense in this context. The wires A and B in positions 3 and 7 were inclined against the probe axis at angles γ_A and γ_B, respectively. Since the corresponding tangential sensitivities k_A and k_B in (14) were dependent on $\tilde{\epsilon}$ and on the mean velocity, a previously measured value of the resultant velocity vector was used to prescribe the dependence of k on $\bar{U}_R$ by interpolation between the calibrated data points. Then $\tilde{\epsilon}$ was approximated by the result of a neighbouring measuring point, the corresponding k was interpolated on the curve $k(\bar{U}_R = \text{const})$ and $\tilde{\epsilon}$ was calculated according to (14). The procedure was repeated several times with a computer; on the average the results did not change after three iterations. The accuracy of measuring $\tilde{\epsilon}$ in this way was checked by means of the calibration device and yielded scatters within $\pm 0{\cdot}5°$. After measuring $\tilde{\epsilon}$ the magnitude of the total velocity was evaluated from either mean voltage $\bar{E}_3$ or $\bar{E}_7$. These results were up to 2 % smaller than those obtained using single hot wires.

For evaluating the Reynolds stresses from the r.m.s. measurements, the directional sensitivities were prescribed according to the local mean flow vector. At each angular hot-wire position (figure 1) the mean-velocity components $\bar{U}_{N1}$ and $\bar{U}_T$ were calculated, and k was interpolated between the calibration points; the cross-flow normal to the plane of the prongs was taken into account with a constant sensitivity $h = 1{\cdot}2$. These sensitivities were inserted in (9) and (10), and the local Reynolds stress tensor was calculated according to the equations of table 1.

2.3. *Accuracy of measured Reynolds stresses*

2.3.1. *Effect of inaccuracies in calibrating the tangential sensitivity k.* During the calibration of the directional sensitivities great care was necessary to avoid misinterpretation of the hot-wire voltages. The effect of small errors in the measured cooling velocity and in the hot-wire angle γ on the tangential sensitivities was analysed from

(12) under the assumption that the hot-wire probe was aligned with the mean-velocity vector, i.e. $\epsilon = \epsilon_0 = 0$ and $\gamma = 90° - \alpha$. The influence of deviations from the actual wire angle γ_r and from the correct cooling velocity $(\overline{U}_c)_r$ was estimated by inserting the perturbation equations $\gamma = \gamma_r + \Delta\gamma$ and $\overline{U}_c/\overline{U}_R = (\overline{U}_c/\overline{U}_R)_r + \Delta(\overline{U}_c/\overline{U}_R)$ into (12) and root-expanding this relation

$$k \simeq k_r - \frac{1}{2}\frac{((\overline{U}_c/\overline{U}_R)^2 - 1)\sin(2\Delta\gamma) - 4\Delta(\overline{U}_c/\overline{U}_R)}{\cos^2\gamma_r}. \tag{15}$$

For an actually calibrated tangential sensitivity $k_r = 0{\cdot}257$ together with $\gamma_r = 45°$ and $\overline{U}_c/\overline{U}_R = 0{\cdot}73$ the relative errors in k were

$$k/k_r - 1 = \mp 0{\cdot}24 \quad \text{for} \quad \Delta\gamma = \pm 1°, \quad \Delta(\overline{U}_c/\overline{U}_R) = 0,$$

$$k/k_r - 1 = \pm 0{\cdot}08 \quad \text{for} \quad \Delta(\overline{U}_c/\overline{U}_R) = \pm 0{\cdot}01, \quad \Delta\gamma = 0.$$

The influence of the errors $\Delta(\overline{U}_c/\overline{U}_R)$ on the tangential sensitivities was kept small. Before and after the eight calibrations with different velocities for one fixed yaw angle α, the calibration curve (11) was checked; deviations due to temperature drift were smaller than 0·5 %, and will be neglected in the following analysis.

From the definition of the cooling velocity $\overline{U}_c = \overline{U}_R(\sin^2\gamma + k^2\cos^2\gamma)^{\frac{1}{2}}$ the perturbations in γ and the corresponding ones in k had no influence on the measured mean velocities. There were, however, effects on the measured Reynolds stresses. The relative errors (r.e. $(x) = x/x_r - 1$) were estimated from the simplified equations (9) and (10) equivalent to those of table 1 but including $\gamma = \gamma_r + \Delta\gamma$ and the corresponding $k^2(\gamma) = k_r^2(\gamma_r) + \Delta k^2(\Delta\gamma)$ for both wires A and B. While terms proportional to $\Delta\gamma_A$ and $\Delta\gamma_B$ were negligible, those containing $\Delta k_A^2(\Delta\gamma_A)$ and $\Delta k_B^2(\Delta\gamma_B)$ were significant. For all stresses of equation system (a) and for $\overline{u_m w_m}$ and $\overline{v_m w_m}$ of system (b) the relative errors were estimated as

$$\text{r.e.}\,(\overline{u_m^2}) = 0, \tag{16}$$

$$\text{r.e.}\,(\overline{v_m^2}, \overline{w_m^2}, \overline{v_m w_m}) = D, \tag{17}$$

$$\text{r.e.}\,(\overline{u_m v_m}, \overline{u_m w_m}) = \tfrac{1}{2}D, \tag{18}$$

with

$$D = \Delta k_A^2 + \Delta k_B^2. \tag{19}$$

If for example the actual tangential sensitivities for two wires were 0·25 and 0·15, and both errors in $\Delta\gamma$ were assumed to be $-2°$, the error D would be 0·1. The corresponding errors in the Reynolds stress tensor according to (16)–(18) were confirmed by recalculating the results of station E5 of I from the same set of measurements with prescribed errors of $\Delta\gamma = \pm 2°$ for both wires. In figure 5 the recalculated data are compared with the actual ones. As indicated by the analysis and the comparison calculations, for the present investigation we could not rely on assumed or effective hot-wire angles, but had to measure the geometrical inclinations instead. Our measurements by means of a microscope and the calibration device scattered within $\pm 0{\cdot}5°$ yielding errors in the Reynolds stresses below $D \simeq \mp 0.04$.

2.3.2. *Effect of empirical values for the tangential sensitivity k.* In many experiments empirical values for the tangential sensitivity k are accepted, while the hot-wire angle is also prescribed. Generally these assumptions are not compatible with the definition (1) of the cooling velocity, and a relative error of approximately $\frac{1}{2}\Delta k^2$ is introduced in the measured mean velocity. Thereby the denominators in (9) and (10) for the Reynolds

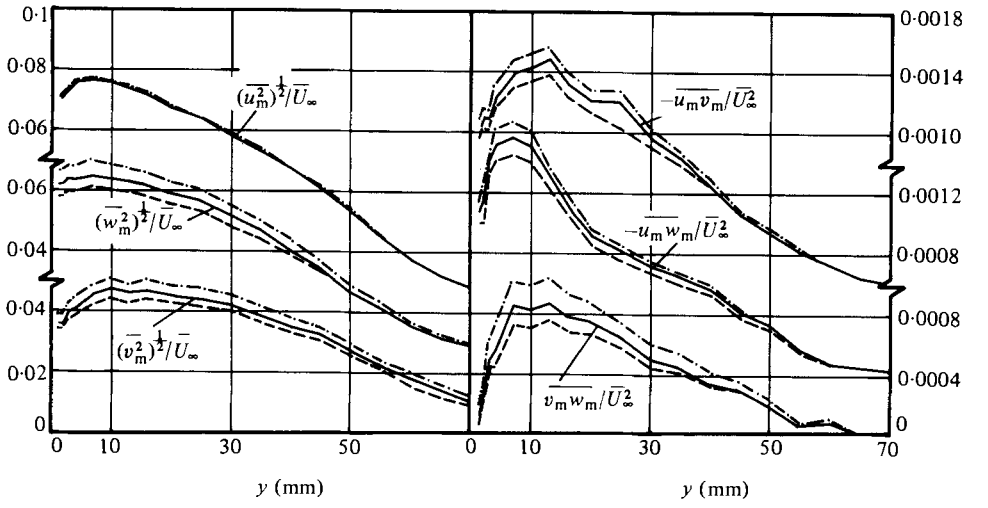

FIGURE 5. Effect of errors in tangential sensitivity k due to errors in hot-wire angle γ_r on measured Reynolds stresses; station E5. -·-·-, $k(\gamma_r - 2°)$; ——, $k(\gamma_r)$; - - -, $k(\gamma_r + 2°)$.

stresses are affected. For this case the relative errors in the measured velocity correlations were estimated in the same way outlined above, but including fixed hot-wire angles $\gamma = \gamma_r = 45°$. With D as defined in (19) we obtained

$$\text{r.e.}\ (\overline{u_m^2}) = -0{\cdot}5D, \tag{20}$$

$$\text{r.e.}\ (\overline{v_m^2}, \overline{w_m^2}, \overline{v_m w_m}) = 1{\cdot}5D, \tag{21}$$

$$\text{r.e.}\ (\overline{u_m v_m}, \overline{u_m w_m}) = 0{\cdot}5D. \tag{22}$$

With these equations the effect of using a cooling law with the tangential sensitivity k instead of one with k_r can be studied. Comparing the cooling law of Webster (1962) and Champagne *et al.* (1967) with $k = 0{\cdot}2$ = constant with the cosine law yields $D = 0{\cdot}08$. The corresponding deviations in the Reynolds stresses are identical with the non-normalized ones of Champagne *et al.*; all relative errors are smaller by $\frac{1}{2}D$ compared with the Reynolds stresses normalized with the cooling velocity.

The deviations in the Reynolds stresses evaluated with the present method compared with those calculated with $k = 0{\cdot}2$ are small for the results of station E5 of I, as can be seen from figure 6, because in the calibrations, as in those of figure 3, Δk_A^2 was approximately equal to $-\Delta k_B^2$, so that the errors cancelled out. However, when this symmetry with respect to the sensitivity of Champagne *et al.* was not present owing to probe or Reynolds-number effects, systematic deviations of more than 10 % arose in the calculated Reynolds stresses.

2.3.3. *Effect of the cross-flow sensitivity h.* Additional to k the sensitivity h of the velocity $\bar{U}_{N2}$ normal to the plane of the hot-wire prongs was taken into account in the data reduction in I. The effect of using the calibrated value $h = 1{\cdot}2$. instead of the ideal one $h = 1$ on the measured Reynolds stresses was checked for those of station E5 of I as shown in figure 6. While all other correlations were insensitive to this change, the crosswise shear stress $\overline{v_m w_m}$ increased up to 15 %. The influence of the sensitivity h on this correlation was estimated from equations corresponding to those of equation

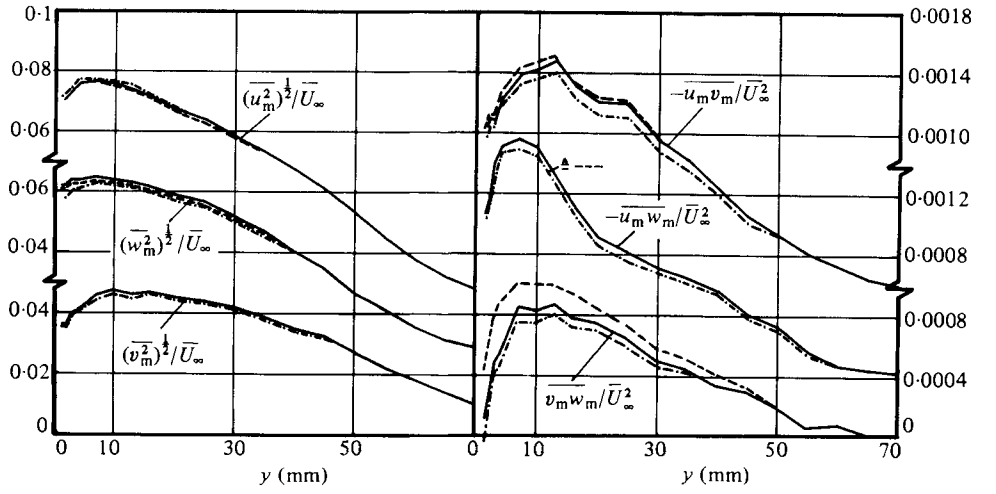

FIGURE 6. Effect of cooling law on measured Reynolds stresses; station E5. —·—·—, $k = 0{\cdot}2, h = 1$ (Champagne *et al.* 1967); ——, $k = k(\overline{U}_R, \alpha)$, $h = 1$; – – –, $k = k(\overline{U}_R, \alpha)$, $h = 1{\cdot}2$ (actual calibrations).

systems (*a*) and (*b*) of table 1; the functions $\overline{F}$, f and g according to (5)–(7) were simplified by $\epsilon = 0$, $\gamma = 45°$ and $k = 0{\cdot}2$. Inserting $h^2 = h_r^2 + \Delta h^2$ in the equations and retaining only the leading terms did not change the results for $\overline{v_m w_m}(b)$ because the errors due to Δh^2 cancelled out. The actual calculations of I deviated slightly from this estimation, the shear stress increased by a few per cent. The accuracy of the correlation $\overline{v_m w_m}(a)$, however, was very sensitive to using $h = 1$ instead of $h_r = 1{\cdot}2$, because all deviations of the $\overline{v_m w_m}$ terms as well as those of the $\overline{u_m w_m}$ terms accumulated. At the measuring station under consideration the relative errors were estimated as

$$\text{r.e.}\,(\overline{v_m w_m}(a)) = \Delta h^2(0{\cdot}1 - 0{\cdot}35\,\overline{u_m w_m}/\overline{v_m w_m}(a)). \tag{23}$$

With the assumption $-\overline{u_m w_m} \geqslant \overline{v_m w_m}(a)$ the relative errors were larger than 20 %. Since the results for $\overline{v_m w_m}$ reported in I were averaged values $\frac{1}{2}[\overline{v_m w_m}(a) + \overline{v_m w_m}(b)]$ the data calculated with $h = 1$ were expected to be underestimated at least by 10 %. This estimation was confirmed by the results of recalculations displayed in figure 6.

The agreement between redundant measurements of the same Reynolds stress was improved considerably by taking into account the calibrated hot-wire response to magnitude and direction of the mean-flow vector. As inferred from the unavoidable scatter of the results, the relative errors were about 10 %, and those of $\overline{u_m w_m}$ and $\overline{v_m w_m}$ were about 10 % of the local $\overline{u_m v_m}$.

3. A method of data reduction for turbulence levels up to 40 %

For measuring the Reynolds stress tensor in a flow with local turbulence levels $Tu = [\frac{1}{3}(\overline{u^2} + \overline{v^2} + \overline{w^2})]^{\frac{1}{2}}/\overline{U}_g \lesssim 0{\cdot}1$ the third-order velocity correlations in the root-expanded equations (9) and (10) cannot be neglected in general. Durst (1971) and Rodi (1975) proposed using the exact time-averaged equation (3), but in practice it is difficult to apply this method for turbulence levels below ~ 40 %, while at higher

turbulence levels reverse flow will probably become significant. Therefore several authors included velocity correlations higher than second order in the root-expanded cooling velocity (e.g. Heskestad 1965; Champagne *et al.* 1967; Vagt 1972, 1979; Bruun 1971*b*, 1972). Vagt (1972) and Heskestad (1965) transformed the third- and fourth-order correlations into second-order ones by assuming certain structures of the velocity field, for example quasi-Gaussian probability distributions. Generally, however, the magnitude and sign of the higher-order moments depend on the flow field considered. Therefore in the present investigation all triple velocity correlations were evaluated from measurements of

$$\overline{\left[\frac{e_n}{S}\right]^3} = \overline{\left[\frac{f_n}{2\bar{F}_n}\right]^3} + O(\overline{u_i^4}), \tag{24}$$

$$\overline{\frac{(e_n \pm e_{n+4})^3}{S^3}} = \overline{\left[\frac{f_n}{2\bar{F}_n} \pm \frac{f_{n+4}}{2\bar{F}_{n+4}}\right]^3} + O(\overline{u_i^4}). \tag{25}$$

The calibrations of the directional sensitivities of each hot wire were taken into account in the functions $\bar{F}$ and f ((5) and (6)). After neglecting fourth-order correlations, those of third order were calculated and used to describe the corresponding terms in (9) and (10), from which the corrected Reynolds stresses were evaluated. The set (26) of equations used is summarized in table 2 after applying the simplifications $\epsilon = \epsilon_0 = k = 0$, $h = 1$, $\gamma = 45°$ in order to show the leading terms.

The method proposed was applied for measuring profiles of the mean velocities, Reynolds stresses and triple velocity correlations in a flow comparable with that of I, but with larger adverse pressure gradients and high turbulence levels in the vicinity

$(\overline{e_7^2} - \overline{e_3^2})/S^2$	$= 2\overline{u_m v_m} + 2\overline{v_m w_m^2}/\bar{U}_g,$	(26–1)
$(\overline{e_5^2} - \overline{e_1^2})/S^2$	$= 2\overline{u_m w_m} + 2\overline{v_m^2 w_m}/\bar{U}_g,$	(26–2*a*)
$(\overline{e_6^2} - \overline{e_8^2} - \overline{e_2^2} + \overline{e_4^2})/S^2$	$= 2\overline{u_m w_m}/T - T(\overline{v_m^3} - \overline{w_m^3})/\bar{U}_g,$	(26–2*b*)
$(\overline{e_2^2} - \overline{e_4^2} + \overline{e_6^2} - \overline{e_8^2})/S^2$	$= 2\overline{v_m w_m} - 4\overline{u_m v_m w_m}/\bar{U}_g,$	(26–3*a*)
$\overline{((e_2 - e_6)^2 - (e_4 - e_8)^2)}/S^2$	$= 4\overline{v_m w_m},$	(26–3*b*)
$\overline{(e_3 + e_7)^2}/S^2$	$= 2\overline{u_m^2} + 4\overline{u_m w_m^2}/\bar{U}_g,$	(26–4)
$\overline{(e_3 - e_7)^2}/S^2$	$= 2\overline{v_m^2},$	(26–5)
$\overline{(e_1 - e_5)^2}/S^2$	$= 2\overline{w_m^2},$	(26–6)
$(\overline{e_2^3} + \overline{e_6^3} - \frac{1}{2}(\overline{e_1^3} + \overline{e_3^3} + \overline{e_5^3} + \overline{e_7^3}))/S^3$	$= 3\overline{u_m v_m w_m}/T,$	(26–7)
$(\overline{e_1^3} + \overline{e_5^3})/S^3$	$= 3\overline{u_m w_m^2}/T + \overline{u_m^3}/T,$	(26–8)
$(\overline{e_3^3} + \overline{e_7^3})/S^3$	$= 3\overline{u_m v_m^2}/T + \overline{u_m^3}/T,$	(26–9)
$(\overline{e_7^3} - \overline{e_3^3})/S^3$	$= \overline{v_m^3}/T + 3\overline{u_m^2 v_m}/T,$	(26–10)
$(\overline{e_5^3} - \overline{e_1^3})/S^3$	$= \overline{w_m^3}/T + 3\overline{u_m^2 w_m}/T,$	(26–11)
$\overline{(e_3 + e_7)^3}/S^3$	$= \frac{1}{4}T\overline{u_m^3},$	(26–12)
$\overline{((e_4 - e_8)^3 - (e_2 - e_6)^3)}/S^3$	$= 2\overline{w_m^3} + 6\overline{v_m^2 w_m},$	(26–13)
$\overline{((e_6 - e_2)^3 + (e_8 - e_4)^3)}/S^3$	$= 2\overline{v_m^3} + 6\overline{v_m w_m^2},$	(26–14)
$\overline{(e_3 - e_7)^3}/S^3$	$= 2T\overline{v_m^3},$	(26–15)
$\overline{(e_5 - e_1)^3}/S^3$	$= 2T\overline{w_m^3}.$	(26–16)

TABLE 2. Set of equations used for evaluating the Reynolds stress tensor and the triple velocity correlations; $T = \sqrt{2}$; simplifications: $\epsilon = \epsilon_0 = k = 0$, $h = 1$, $\gamma = 45°$

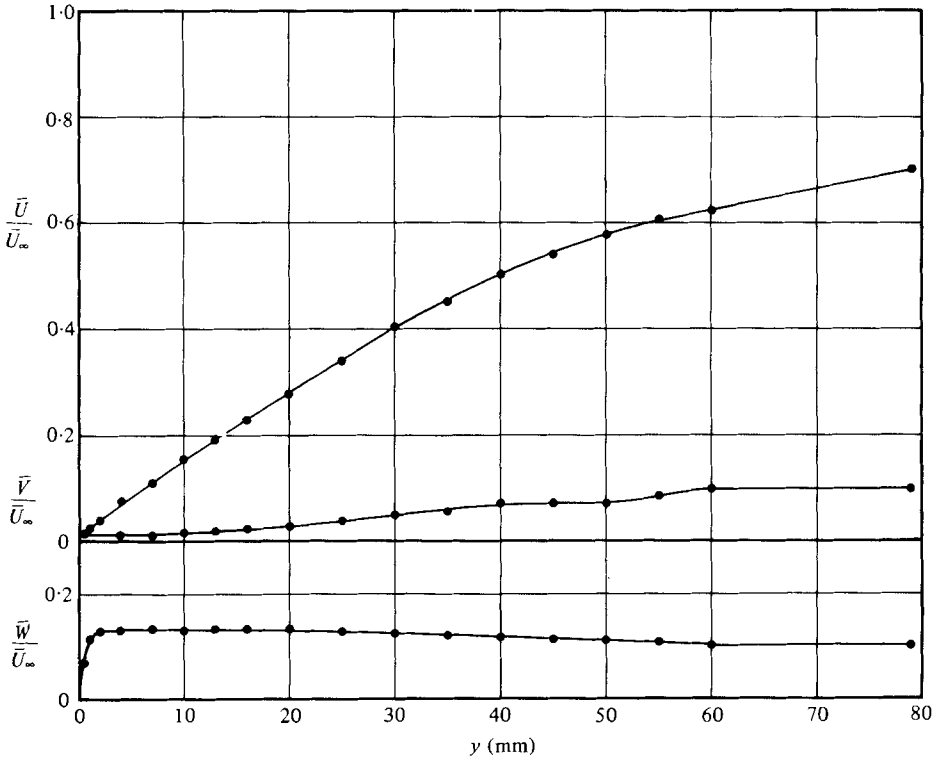

FIGURE 7. Mean velocities in the vicinity of separation; measured in a flow field comparable with that of I. station E3, $Re = 1{\cdot}5 \times 10^6$, $c_p = 0{\cdot}59$.

of separation (figures 7–9). The mean-velocity components $\bar{U}$ and $\bar{W}$ of figure 7 are defined in a Cartesian co-ordinate system, the x-axis of which is approximately aligned with the wind-tunnel centre line; the vertical velocity $\bar{V}$ is identical with $\bar{V}_m$. At the measuring station chosen the turbulence levels increased from $Tu \simeq 0{\cdot}2$ at $y = 25\,\text{mm}$ to $Tu \simeq 0{\cdot}35$ at $y = 4\,\text{mm}$. The Reynolds stresses evaluated according to the equation system of table 2 are compared in figure 8 with those calculated from the same set of data using the conventional linearized method. Though the accuracy of the third-order moments measured with analogue equipment was limited by errors up to $\pm 10\,\%$ in $\overline{e_n^3}$ and $\overline{(e_n \pm e_{n+4})^3}$, the magnitude of the corrections is obvious from the comparison. In these calculations the time-averaged cooling velocity measured with a single normal-wire probe was iteratively corrected by including the second-order correlations according to (8):

$$\bar{U}_c = \bar{U}_g\left(1 + \frac{1}{2}\frac{\overline{v_m^2}}{\bar{U}_g^2} + \frac{k^2\overline{w_m^2}}{\bar{U}_g^2}\right). \tag{27}$$

The results of figures 8 and 9 show that the corrected $\overline{u_m^2}/\bar{U}_\infty^2$ correlation was reduced up to 14 % by the term $2(\overline{u_m w_m^2}/\bar{U}_\infty^3)/(\bar{U}_g/\bar{U}_\infty)$ according to (26–4). The shear stress $\overline{v_m w_m}$ as estimated from (26–3a) increased about 15 % at $y = 7\,\text{mm}$ due to a positive correlation $(u_m v_m w_m/U_\infty^3)/(U_g/U_\infty)$; the influence of this term increased rapidly with decreasing resultant mean velocity $\bar{U}_g$. The calculation of $\overline{v_m w_m}$ according to (26–3b), however, was approximately independent of the triple velocity correlations, so the resultant deviations indicated in figure 8 were about half the corrections corresponding

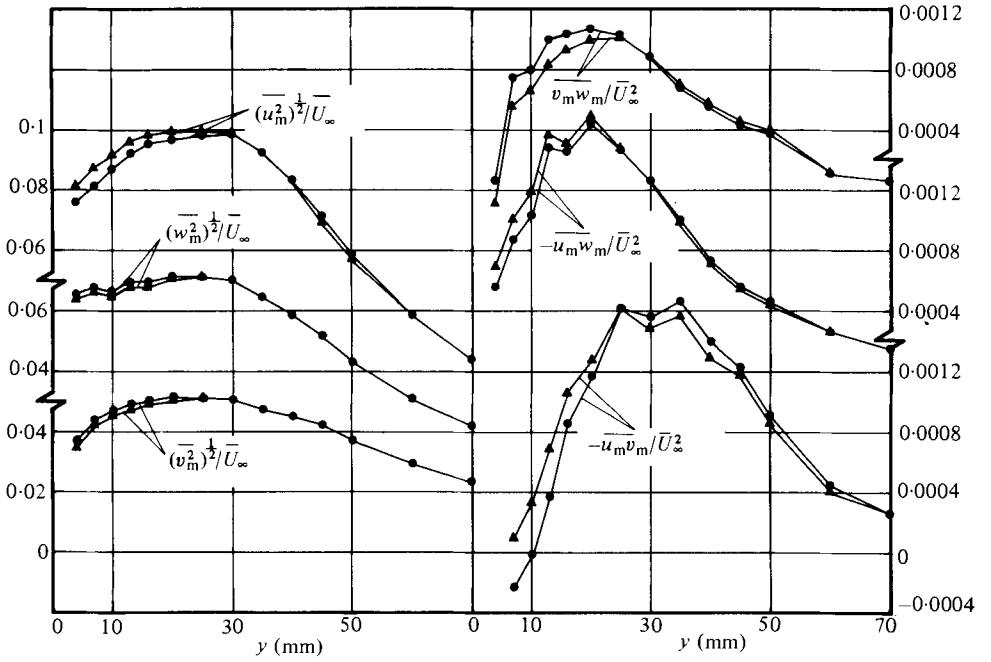

FIGURE 8. Evaluation of Reynolds stresses with conventional method (▲) and that proposed here (●). station E3, $Re = 1{\cdot}5 \times 10^6$, $c_p = 0{\cdot}59$.

to (26–3a). The Reynolds shear stress $\overline{u_m v_m}$ evaluated with the present method was dependent on $(\overline{v_m w_m^2}/\bar{U}_\infty^3)/(\bar{U}_g/\bar{U}_\infty)$. In the inner region of the boundary layer the results were smaller than those calculated with the conventional method; in the outer layer they were slightly larger.

The results of the test measurements (figure 8) indicated that for the flow field investigated the triple correlations had a non-negligible effect on the calculated Reynolds stresses for $y \lesssim 25$ mm with $Tu > 0{\cdot}2$; for $y > 25$ mm with $Tu < 0{\cdot}2$ the third-order terms are negligible. Since the highest turbulence level encountered in I was 23 %, the use of the conventional linearized method for evaluating the Reynolds stresses was justified.

4. Concluding remarks

In the boundary-layer experiment described in I profiles of the Reynolds stress tensor were measured with inclined hot-wire probes, which were aligned with the local yaw direction and were rotated around the probe axis. We used the DISA miniature X-wire probe 55P61 and platinum–tungsten wires with $d = 5\,\mu$m and $l = 1{\cdot}2$ mm. Preliminary investigations revealed large scatter up to 40 %, especially for the cross-flow shear stress $\overline{v_m w_m}$, when carrying out repeated measurements with several probes of the same type. We found that the directional response of the hot wires could not be described by a single empirical cooling law. Therefore an effective cooling velocity defined in (1) was used to describe the wire cooling; the sensitivities k and h with respect to the velocity components tangential to the wire or normal to the plane of the prongs, respectively, were calibrated individually for each

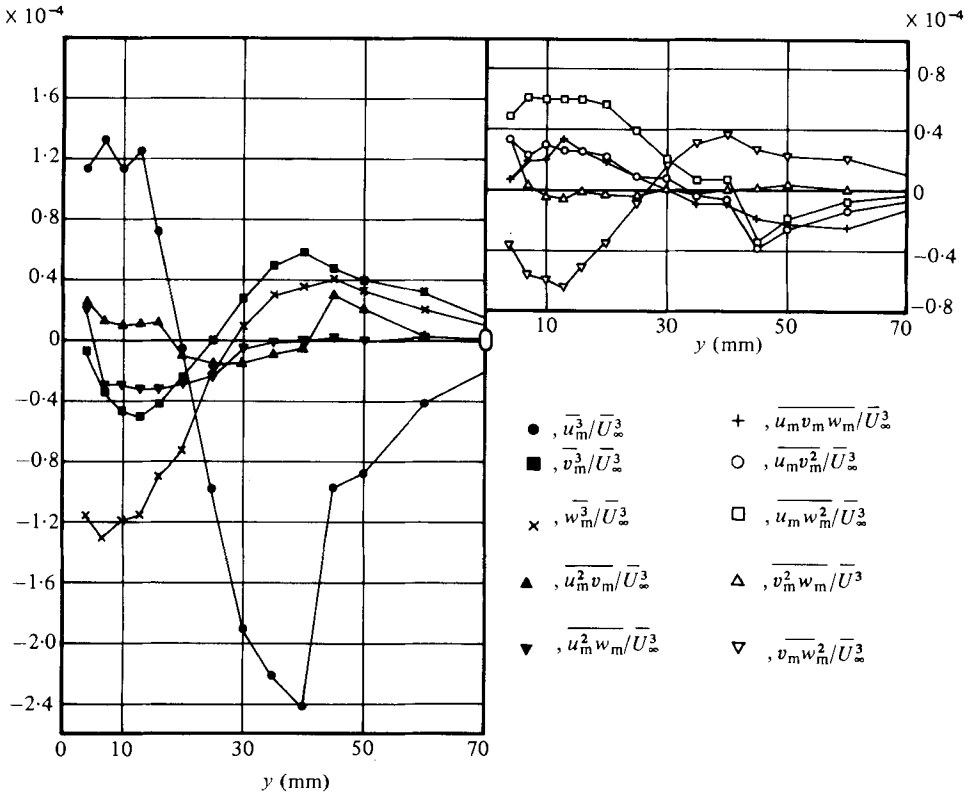

FIGURE 9. Measured triple velocity correlations. station E3, $Re = 1{\cdot}5 \times 10^6$, $c_p = 0{\cdot}59$.

hot wire used. In general the tangential sensitivity k decreased with increasing angle between the velocity vector in the plane of the prongs and the wire normal, and was also dependent on the magnitude of the velocity. Therefore measurements of flow directions required an iterative evaluation procedure. The cross-flow sensitivity h calibrated for the flow conditions encountered in I was approximately $h = 1{\cdot}2 =$ constant. For evaluating the Reynolds stresses from the measurements obtained at a prescribed angular position of the hot-wire probe, the tangential sensitivity k was interpolated between the calibrated data points using those components of the local mean-velocity vector lying in the plane of the hot-wire prongs, while the velocity component normal to that plane was taken into account with $h = 1{\cdot}2$.

The geometrical angle between a hot wire and the probe axis had to be measured accurately, because deviations from this value influenced the sensitivity k obtained from the calibrations and thus impaired the results for the Reynolds stresses. An error analysis indicated that inaccuracies of 0·5° encountered in our measurements of the wire angles yielded relative errors up to 12 % for k and 4 % for the Reynolds stresses.

Additionally the effect of presuming the wire angles to be known and simultaneously using an empirical value for the tangential sensitivity k different from the true one was analysed from the governing equations. The assessment by Champagne *et al.* (1967) of the relative errors in the measured Reynolds stresses evaluated with their value $k = 0{\cdot}2 =$ constant as opposed to the cosine law was reconfirmed. The comparison

between the present results, which were obtained by incorporating the calibrated tangential sensitivities, and those evaluated with $k = 0{\cdot}2$ indicated vanishing differences, if the arithmetical average of the sensitivities of both hot wires of an X-probe was equal to the value found by Champagne *et al.* Likewise, whenever this symmetry was not present owing to probe or Reynolds-number effects, deviations above 10 % in the calculated Reynolds stresses were encountered. The analytical error analysis was confirmed by corresponding recalculations of the velocity correlations using the measurements of station E5 of I and applying different cooling laws in the data reduction.

Since with the probe support used the longitudinal probe axis could not be aligned with the local pitch direction of the resultant velocity vector, a mean-velocity component normal to the plane of the wires was encountered during rotation of the probe. By taking into account this velocity and the corresponding fluctuation with the ideal sensitivity $h = 1$ instead of the calibrated value $h = 1{\cdot}2$ all Reynolds stresses calculated from equation system (*b*) of table 1 remained unchanged because the errors cancelled out; the crosswise shear stress $\overline{v_m w_m}$, however, determined from system (*a*) was underestimated by 20 % at the measuring station considered. Generally the data reduction, including the calibrated directional sensitivities of each hot wire used, improved the accuracy of the Reynolds stresses obtained from repeated measurements to relative errors within $\pm$ 10 %, the accuracy for the shear stresses $\overline{u_m w_m}$ and $\overline{v_m w_m}$ was estimated as 10 % of $\overline{u_m v_m}$.

In I measurements in the vicinity of separation had to be excluded because the local turbulence levels increased with decreasing magnitudes of the mean velocity vectors. The upper limit for using the conventional linearized method for evaluating the Reynolds stress tensor from the root-expanded equation for the cooling velocity was estimated from tests by including all measured triple velocity correlations in the data reduction and comparing the calculated Reynolds stresses with those evaluated conventionally. The comparison showed that in the flow field investigated the linearized method would overestimate the correlations $\overline{u_m^2}$ and $|\overline{u_m v_m}|$, while $|\overline{v_m w_m}|$ calculated from (26–3*a*) would be too low when turbulence levels exceeded approximately 20 %; the shear stress $v_m w_m$ determined from (26–3*b*) was unaffected by triple velocity correlations. The results of the test measurements validated the conventional data reduction applied in I.

The proposed method of including triple velocity correlations allows for measurements of Reynolds stresses with conventional accuracy in flows with turbulence levels up to about 40 %, as long as instantaneous reverse flow is not significant. The data, however, should be advantageously measured by a triple-wire probe and be processed by a minicomputer so that the calculation of the resultant instantaneous velocity vector can incorporate the calibrated directional sensitivities of the hot wires used.

REFERENCES

BERG, B. v. D. & ELSENAAR, A. 1972 Measurements in a three-dimensional incompressible turbulent boundary layer in an adverse pressure gradient under infinite swept wing conditions. *NLR Tech. Rep.* no. 72092 U.

BRADSHAW, P. 1972 The understanding and prediction of turbulent flow. *Jahrbuch der Deutschen Gesellschaft für Luft- und Raumfahrt*, p. 51.

BRUUN, H. H. 1971*a* Interpretation of a hot-wire signal using a universal calibration law. *J. Phys.* E: *Sci. Instrum.* **4**, 225.

BRUNN, H. H. 1971*b* Linearisation and hot-wire anemometry. *J. Phys.* E: *Sci. Instrum.* **4**, 815.

BRUUN, H. H. 1972 Hot-wire data corrections in low and high turbulence intensity flows. *J. Phys.* E: *Sci. Instrum.* **5**, 812.

BRUUN, H. H. 1975 Interpretation of X-hot-wire signals. *DISA Info.* no. 18, p. 5.

CHAMPAGNE, F. H., SLEICHER, C. A. & WEHRMANN, O. H. 1967 Turbulence measurements with inclined hot-wires. Part 1 and 2. *J. Fluid Mech.* **28**, 153.

DECHOW, R. 1977 Mittlere Geschwindigkeit und Reynoldsscher Spannungstensor in der dreidimensionalen turbulenten Wandgrenzschicht vor einem stehenden Zylinder. In *Strömungsmechanik und Strömungsmaschinen*, Heft 21. Mitteilungen des Instituts für Strömungslehre und Strömungsmaschinen, Univ. Karlsruhe.

DURST, F. 1971 Evaluation of hot-wire anemometer measurements in turbulent flows. *Imperial College, Dept Mech. Engng Rep.* ET/TN/A/9.

ELSENAAR, A. & BOELSMA, S. H. 1974 Measurements of the Reynolds stress tensor in a three-dimensional turbulent boundary layer under infinite swept wing conditions. *NLR Tech. Rep.* no. 74095 U.

FRIEHE, C. A. & SCHWARZ, W. H. 1968 Deviations from the cosine law for yawed cylindrical anemometer sensors. *Trans. A.S.M.E.* E, *J. Appl. Mech.* **35**, 655.

HFSKESTAD, G. 1965 Hot-wire measurements in a plane turbulent jet. *Trans. A.S.M.E.* E, *J. Appl. Mech.* **32**, 721.

HINZE, J. O. 1975 *Turbulence.* McGraw-Hill.

HORVATIN, M. 1970 A contribution to the calibration of hot-wire dual probes. *DISA Info.* no. 10, p. 22.

IRWIN, H. P. A. H. 1971 The longitudinal cooling correction for wires inclined to the prongs and some turbulence measurements in fully developed pipe flow. *McGill Univ., Montreal, Mech. Engng Res. Lab. Tech. Note* no. 72–1.

JOHNSTON, J. P. 1970 Measurements in a three-dimensional turbulent boundary layer induced by a swept, forward facing step. *J. Fluid Mech.* **42**, 823.

JÖRGENSEN, F. E. 1971 Directional sensitivity of wire and fiber-film probes. *DISA Info.* no. 11, p. 31.

KJELLSTRÖM, B. & HEDBERG, S. 1970 Die Eichung eines DISA Hitzdrahtanemometers und Bestätigung der Eichung durch Messung in einem zylindrischen Kanal. *DISA Info.* no. 9, p. 8.

KRAUSE, E. 1974 Analysis of viscous flow over swept wings. *ICAS Paper* no. 74–20.

KRAUSE, E. 1975 Flow analysis through numerical techniques. In *AGARD* LS 73.

MARVIN, J. G. 1977 Turbulence modeling for compressible flows. *NASA Tech. Memo.* X-73, 188.

MÜLLER, U. R. 1982 Measurements of the Reynolds stresses and the mean-flow field in a three-dimensional pressure-driven boundary layer. *J. Fluid Mech.* **118**, 121.

MÜLLER, U. R. & KRAUSE, E. 1979 Measurements of mean velocities and Reynolds stresses in an incompressible three-dimensional turbulent boundary layer. In *Proc. 2nd Symp. on Turbulent Shear Flows, Imperial College, London*, p. 15.36.

RODI, W. 1975 A new method for analysing hot-wire signals in highly turbulent flows, and its evaluation in a round jet. *DISA Info.* no. 17, p. 9.

ROTTA, J. C. 1977 A family of turbulence models for three-dimensional thin shear layers. In *Proc. 1st Symp. on Turbulent Shear Flows, Pennsylvania State Univ.*, p. 10.27.

VAGT, J. D. 1972 Hot-wire measurement techniques in a highly turbulent flow and the calculation of intensities. In *Heat and Mass Transfer in Boundary Layers (Proc. Int. Summer School Heat and Mass Transfer in Turbulent Boundary Layers, Herceg Novi, Sept. 1968, and selected papers and abstracts of the International Seminar Heat and Mass Transfer in Flows with Separated Regions, Herceg Novi, Sept. 1969)* (eds. N. Afgan, Z. Zaric & P. Anastasijevic), vol. 2, p. 995, Pergamon.

VAGT, J. D. 1979 Hot-wire probes in low speed flow. *Prog. Aero. Sci.* **18**, 271.

WEBSTER, C. A. G. 1962 A note on the sensitivity to yaw of a hot-wire anemometer. *J. Fluid Mech.* **13**, 307.